

Article

CO₂ Emission of Electric and Gasoline Vehicles under Various Road Conditions for China, Japan, Europe and World Average—Prediction through Year 2040

Xue Dong ¹, Bin Wang ², Ho Lung Yip ³  and Qing Nian Chan ^{3,*}

¹ China-UK Low Carbon College, Shanghai Jiao Tong University, Shanghai 200240, China; xue.dong@sjtu.edu.cn

² State Key Laboratory of Ocean Engineering, School of Naval Architecture, Ocean & Civil Engineering, Shanghai Jiao Tong University, Shanghai 200240, China; wangbin1981525@sjtu.edu.cn

³ School of Mechanical and Manufacturing Engineering, University of New South Wales, Sydney, NSW 2052, Australia; h.l.yip@unsw.edu.au

* Correspondence: qing.chan@unsw.edu.au

Received: 29 March 2019; Accepted: 29 May 2019; Published: 4 June 2019



Abstract: Many countries are making strategic plans to replace conventional vehicles (CVs) with electric vehicles (EVs), with the motivation to curb the growth of atmospheric CO₂ concentration. While previous publications have mainly employed social-economic based models to predict CO₂ emission trends from vehicles over the years, they do not account for the dynamics of engine and motor efficiency under different driving conditions. Therefore, this study utilized an experimentally validated vehicle dynamic model to simulate the consumption of gasoline and electricity for CVs and EVs, respectively, under eight driving cycles for different countries/regions. The CO₂ emissions of CVs and EVs through 2040 were then calculated, based on the assumptions of the improvement of engine efficiency and composition of power supply chain over the years. Results reveal that, assuming that the current projections and assumptions remain valid, China would have the highest CO₂ emission for EVs, followed by Japan, world average and the EU, mainly determined by the share of fossil fuels in the power grid. As for the influence of road conditions, the CO₂ emission of CVs was found to be always higher than that of EVs for all countries/regions over the years. The difference is around 10–20% under highway conditions, and as high as 50–60% in crowded urban driving conditions.

Keywords: CO₂ emission; gasoline vehicles; electric vehicles; driving cycles; vehicle dynamic model

1. Introduction

An increasing level of anthropogenic greenhouse emissions is considered to have significant impacts on the climate and marine environment [1]. As the adverse effects of climate change are leaving some countries vulnerable in terms of quality of life, physical infrastructure and biological diversity, etc. [2], the international community has been increasingly active in response to climate challenges in recent years [3]. For example, the Paris Agreement aims to control the increase in the global average temperature to well below 2°C above pre-industrial levels [4]. In order to achieve this long-term temperature goal, parties of the Paris Agreement aim to reach global peak greenhouse gas emissions as soon as possible, so as to achieve a balance between anthropogenic emissions of greenhouse gases by sources and removals by sinks in the second half of this century [5]. Of all the greenhouse gases, CO₂ is the major concern as it is the most abundant composition. Atmospheric CO₂ stabilization target at 450 ppm would be needed to forestall coral reef bleaching, thermohaline circulation shutdown, and sea level rise from disintegration of the West Antarctic Ice Sheet [6]. However, achieving such

target would require significant effort, and even stabilizing atmospheric CO₂ concentration at 550 ppm requires a carbon-free energy usage of 15 TW by mid-21st century [6]. The current global annual energy usage is around 20 TW, with 82% of the energy consumption being supplied from non-carbon-neutral sources [7]. It can therefore be anticipated that, without effective measures to limit CO₂ emissions, it will be challenging to achieve the emission targets set by the Paris Agreement.

1.1. The Contribution of Road Traffic Emissions to Global Greenhouse Gas Emissions

Transportation has become a significant contributor to the global energy crisis and high greenhouse gas emissions. In 2006, 60.5% of the world's petroleum was consumed in cars, and this figure is anticipated to reach 62% by 2020 [8]. High consumption rate of fossil fuels is accompanied with a considerable amount of CO₂ emission. Specifically from 2001 to 2011, CO₂ emissions increased by 13%, and 25% of this increase is attributed to vehicle emissions [8]. Given that internal combustion engine is still the major powertrain system for on-road vehicles, many countries are making strategic plans to replace the conventional vehicles (CVs) with electric vehicles (EVs) and fuel cell vehicles with lower tailpipe emissions, in an effort to curb CO₂ emissions. For instance, the US government enacted energy policy provisions to support the development of hydrogen energy and fuel cell technologies in 2003. In 2009, the US also announced plans to achieve 1 million plug-in hybrid vehicles on the road by 2015 [8]. Similarly, Germany issued the national electro-mobility development plan in 2009, and it declared plans to have at least 1 million EVs by 2020 and 5 million by 2030 [9], with the investment of 5 billion euros (~5.6 billion USD) in hydrogen energy and fuel cell technology development from 2007 to 2017 [8]. In addition, the Japanese government planned to build 8500 hydrogen refueling stations by 2030 [8] and it is estimated that the country's fuel cell vehicles will account for 20% of the total vehicles on the road by that time [8]. Meanwhile, China became the country with the highest CO₂ emissions and energy consumption in 2006 and in 2009, respectively [10]. At the same time, China's transportation industry is still dominated by internal combustion engine vehicles (i.e., 62.39% of railway locomotives, 84.42% of civilian transport ships, and 98.93% of civilian motor vehicles) [8]. In order to alleviate these problems, China's central and local governments have taken extensive measures in recent years [11], including the introduction of more stringent fuel consumption regulations [12], subsidy scheme to accelerate penetration of the electric vehicle market [13], and restrictions on the purchase of vehicles and license plates, etc. [14]. Therefore, replacing CVs with EVs and FCVs seems to be an inevitable trend worldwide.

1.2. The CO₂ Emission from CV, EV and HEV of Different Countries/Regions

The CO₂ emission of EV and hybrid electric vehicle (HEV), however, varies among countries/regions, due to the difference in the composition of power grid. According to Howey et al. [15], HEV showed the the lowest CO₂ emission, with more than half of the tested HEVs had an emission of 70 g CO₂/km, while that for most of the tested EVs were 70–110 g CO₂/km. The most efficient diesel engine vehicles, however, were reported to have the highest emission exceeding 110 g CO₂/km, despite the recent development of diesel fuel and injection strategy [16–18]. It is worth noting that these results were acquired based on the structure of British power grid, where CO₂ emission rate is 542 g CO₂/kWh. Similarly, Sullivan et al. [19] suggested that EV consumes less energy per kilometer compared with CV, but it was also identified that EV is not comparable with CV with regard to dynamic power and cruising range. In addition, Samaras and Meisterling [20] studied the life-cycle CO₂ emission of HEVs in the US, and their results revealed that HEV has lower emission than CV only when the power grid uses sufficient renewable energy. As coal-fired plants powered most of the grids in China, the CO₂ emission rate of EVs in China is higher than that of other developed countries. A previous study by Hao et al. [21] reported that the collective use of five control measures in China, including constraining vehicle registration, reducing vehicle travel, strengthening fuel consumption rate limits, vehicle downsizing and promoting EV penetration, will reduce energy consumption by 62.9% and 75.7%, by 2030 and 2050, respectively, when compared with the reference

scenario with no measures taken in China. In the same study, it was also reported that similar potential in greenhouse gas mitigation can be realized. Likewise, Peng et al. [22] analyzed the CO₂-reduction potentials and emissions abatement costs from micro-vehicular and macro-industrial perspectives from 2010 to 2030, and found that the technologies with large emissions reduction potential are mainly available in plug-in hybrid electric vehicle (PHEV) and EV paths, which would be the main channels for reducing carbon emissions in the long run. While the carbon emission of CV, EV and HEV has been studied and reported by researchers from different countries, there is, however, no direct and fair comparison reported about the well-to-wheel CO₂ emission of CV and EV among different countries/regions, which this paper seeks to address.

1.3. The Effect of Road Conditions on Vehicle CO₂ Emission

Although previous social-economic based research model using macroscopic social-economic data, e.g., national-average sales, ownership and oil consumption, etc. provides valuable predictions on the emission trends over the years, results acquired from vehicle dynamic models are also desired because CO₂ emission is highly dependent on engine/motor efficiency, hybrid extent and road conditions, etc., which have to be obtained from vehicle dynamic models. Other institutes, such as Argonne National Laboratory, have previously developed the Powertrain Systems Analysis Toolkit (PSAT) to simulate vehicle efficiency and cycle implications over different of driving cycles [23]. Further work, however, is required to estimate CO₂ emissions of CVs and EVs in the future under the combined effects of driving cycles and energy utilizations, which is the motivation behind this study.

Driving cycles, which determine the relationship between vehicle speed and time, are produced by different countries and organizations to assess the performance of vehicles under real-life road conditions. For example, US06, high way fuel economy test (HWFET) cycle, urban dynamometer driving schedule (UDDS) cycle and New York City Cycle (NYCC) were formulated by the US Environmental Protection Agency [24], while new European driving cycle (NEDC) and JC08 are from Europe and Japan, respectively. Development and Reform Commission of China formulated urban test cycles with Chinese characteristics, including Chinese city driving cycle for urban road (CCUR) and Chinese city driving cycle for the expressway (CCEW) [25]. These driving cycles were originally used to measure exhaust emissions from CVs and are currently being employed to assist in the analysis, design and testing of EVs as well. More detailed information about these drive cycles will be provided in Section 2.4.

This current study aims to predict the well-to-wheel emission of gasoline fuelled CVs and EVs of different countries/regions under various driving conditions. The prediction is made from year 2018 through year 2040 because this is the time frame for which International Energy Outlook provided detailed information about energy utilization of different countries.

2. Methodology

2.1. CO₂ Emission of Electricity and Gasoline

In this work, the well-to-wheel, i.e., well-to-tank plus tank-to-wheel CO₂ emission of CV and EV was predicted. It is worth noting that, while this study accounts for the carbon emission from battery manufacturing and waste recovery, the CO₂ emission of car manufacturing and that is induced by the increased infrastructure for power supply are not considered. In this study, the well-to-wheel CO₂ emission was calculated using a vehicle dynamic model, which incorporates a spark-ignition direct-injection (SIDI) gasoline engine, a motor, battery and transmission system. The SIDI gasoline engine was chosen because it is the mainstream technology due to its improved fuel economy, more precise air-fuel ratio control and improved transient response [26–30].

The well-to-tank CO₂ emission of gasoline, i.e., carbon emission during the mining, storage and transportation process, is estimated to be 406.8 g/L [31]. The well-to-wheel CO₂ emission of gasoline vehicle is calculated to be 2.734 kg/L, with the CO₂ emission regulation and fuel consumption assumption of 128 g/km and 5.5 L/100 km, respectively. This emission level will be applied together with the fuel consumption calculated in the next section, to predict the CO₂ emission of gasoline vehicles over the years.

The CO₂ emission of EV mainly depends on the emission of power, as well as the carbon emission from battery manufacturing and waste recovery. According to Samaras and Meisterling [20], approximately 1510–1870 MJ of primary energy is required during the manufacturing process of 1 kWh of Li-ion battery storage capacity and its materials. Therefore, the average value of 1700 MJ or 10 g CO₂-eq/km was estimated as the carbon impacts of battery over the vehicle life-cycle from that of lithium-ion battery. The carbon emission of power is determined by the composition of the power grid because different forms of power generation result in different levels of CO₂ emission, as shown in Figure 1 [31].

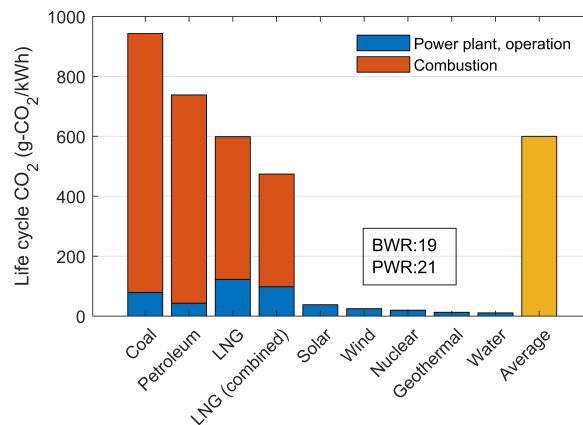


Figure 1. Life-cycle CO₂ emission from different forms of power generation [31]. BWR and PWR are abbreviations for boiling water reactor and pressurized water reactor, respectively.

Based on the life-cycle CO₂ emission of different forms of power generation shown in Figure 1, and the composition of power grid of different countries/regions reported in International Energy Outlook 2017 [7], the CO₂ emission of electricity (g/kWh) for the world average, EU, China and Japan can therefore be estimated, as shown in Figure 2. These countries/regions were chosen in this study as China and the EU are two extreme cases, representing the highest and lowest CO₂ emission per kWh of electricity generated, respectively, while that of Japan and World Average are in the middle. It can be seen from year 2018 to 2040 that the overall CO₂ emission of electricity is projected to decrease over the years for all countries/regions studied, as a result from the anticipated increase in the share of renewables with lower carbon emissions in all power supply chains. Of the individual countries/regions studied, China has the highest CO₂ emission per kWh of electricity generated due to its large share of coal-fired power, while the EU has the lowest over the years. The world average CO₂ emission level is in between the EU and China, whilst Japan has an emission level slightly higher than the world average over the 32-year projection. These data, when combined with the electricity consumption of EVs calculated in the following section, can be used to project the CO₂ emission of EVs for different countries/regions through 2040.

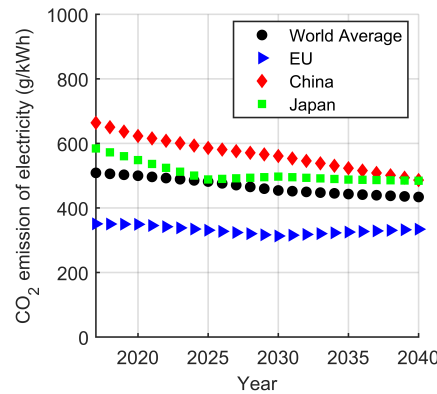


Figure 2. CO₂ emission per kWh of electricity generated for different countries/regions calculated according to International Energy Outlook 2017 [7].

2.2. Vehicle Dynamic Model

The vehicle dynamic model is usually employed to simulate the overall performance of vehicle during the design and optimization process. In this work, a PHEV was studied because it is the most common type of HEV and it can run purely as a gasoline fuelled CV or a EV. As shown in Figure 3, the model consists of the power sources (engine and motor), the transmission systems (P2 clutch, Dual Clutch Transmission (DCT)), battery, vehicle and the driver module. The control strategy can be divided into three modules—driving mode identification module, required torque calculation module and driving mode actuation module. Together with the vehicle dynamic model, different driving modes can be achieved, which enables quantitative analysis on energy consumption under various driving modes, thus optimizing the energy management strategy. The vehicle model in the current study employs forward simulation. This means that the actuation starts from the driver, who can sense the speed of vehicles and adjust its speed accordingly. The action generates torque in the powertrain, and the torque is subsequently transmitted to the wheels. A flow diagram of the vehicle dynamic model employed in this study is presented in Figure 4, and the details of each submodule are discussed from Sections 2.2.1–2.2.7.

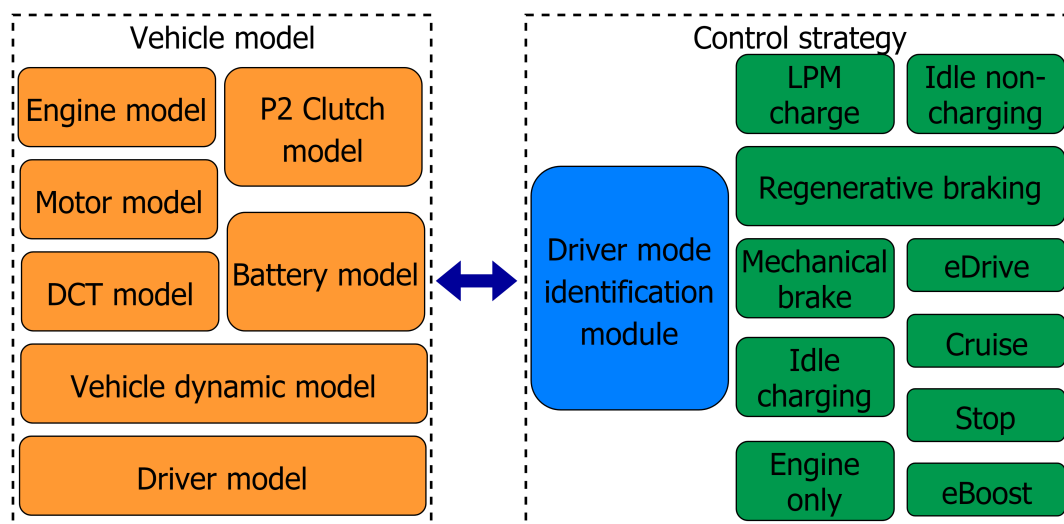


Figure 3. Structure of the vehicle dynamic model and its control strategy.

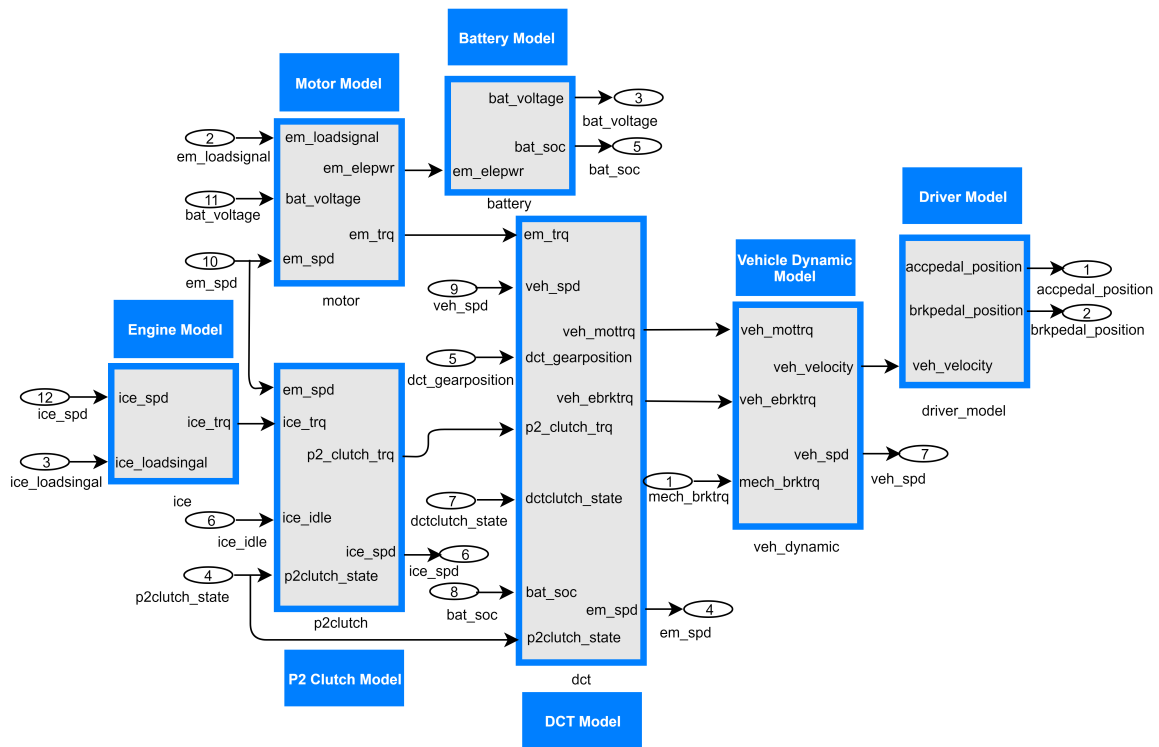


Figure 4. Flow diagram of the vehicle dynamic model of a hybrid electric vehicle employed in this study.

2.2.1. Engine Model

In the HEV dynamic model, only the input and output of the engine are considered. As such, the engine performance under different operating conditions can be acquired from the engine characteristic curve (shown later in Section 2.3). The input operating parameters include the engine speed and control signal, while the output signal is engine torque. Specifically, when the control signal is higher than zero, the fuel consumption rate is calculated based on the engine speed and torque; while the control signal equals to zero, the fuel consumption rate is determined by that in idle conditions.

2.2.2. Motor Module

The motor module is to convert the required vehicle speed and torque to the required battery power, and then generates the corresponding torque based on the battery capacity. The motor model was established based on the motor voltage, torque, power and operating characteristic equation. With torque and power being the outputs, the input is the speed connected to the transmission system and motor control signal. When the signal is positive, the motor is actuated, and the motoring torque was calculated based on the motor speed, control signal and voltage of the battery; whereas, when the control signal is negative, the transmission system drives the motor to regenerate electricity. The power P_m under motoring and regenerating condition follows Equation (1). The electricity transmission losses from both the motor control unit (MCU) and the motor itself were taken into account by experimentally testing the efficiency of the motor system (i.e., motor body + motor controller) under different working modes. The data acquired was then applied in the model. An equivalent battery charging efficiency of 98% was also used to account for the losses from battery charging and conversion from AC to DC:

$$P_m = \begin{cases} \frac{T_m \omega_m}{\eta_m} & \text{motoring,} \\ T_m \omega_m \eta_m & \text{regenerating,} \end{cases} \quad (1)$$

where η_m is motor efficiency, ω_m is the motor rotating speed connected with the transmission system, and T_m is the motor torque.

2.2.3. P2 Clutch Model

The inputs to the clutch model include the engine torque, rotation speed connected to the transmission system, the working conditions of the P2 clutch, and the engine speed in idle conditions. The outputs are the transmission torque of the clutch as well as the engine speed. While the P2 clutch is engaged, the speed and transmission torque of the engine is the same as those of the motor; however, when the P2 clutch is disconnected, the engine remains in an idle condition, as such the transmission torque of the clutch is zero.

2.2.4. Battery Model

The battery model describes the mathematical relationship among the voltage, current, resistance, temperature and state of charge (SOC). The current study employed the internal resistance battery model, for which the input is the discharge power of the battery, and the model outputs are voltage and SOC.

2.2.5. DCT Model

In the DCT model, the input parameters include the motor torque, P2 clutch torque, rotating speed of the wheel, DCT gear position, DCT state, P2 clutch state, and SOC, while the output parameters include the torque transmitted to the wheel, brake recovery torque, and motor speed. When the transmission torque is positive, the vehicle is driven by the power source; otherwise, the vehicle is under brake state, where the recovery torque is calculated. When the DCT is engaged, the motor speed was determined by the wheel speed. However, while the DCT is disconnected, the motor idle speed was determined through SOC.

2.2.6. Vehicle Dynamic Model and Driver's Model

The inputs of the vehicle dynamic model include driving torque, mechanical braking torque and brake recovery torque, and the outputs of this module are vehicle speed and wheel rotating speed. The driver's model can be approximated as a vehicle speed controller. This model employed a proportional–integral–derivative (PID) controller, where the difference between the expected driving speed and the actual vehicle speed is converted to the acceleration or deceleration command. Specific for the current study, the instantaneous command was given based on the speed and torque required by the driving cycle.

2.2.7. Control Strategy

Ten working modes of the current HEV model and their specifications, including `veh_stop`, `idle_nocharging`, `idle_charging`, `brk_disablebrking`, `brk_enablebrking`, `cruise`, `eDrive`, `low power mode (LPM) charging`, `eBoost` and `ice_alone`, are listed in Table 1. Figure 5 shows the flow diagram of control strategy. From the perspective of energy management, the control strategy aims to provide optimized working condition for the engine. Therefore, baseline control strategy was used. The baseline control restricts the engine to work under its high efficiency regime by setting threshold of the operating conditions. In this strategy, the motor was flexibly utilized as an assistant power source whenever the power from engine itself is insufficient, thus achieving “peak clipping” for the engine.

Table 1. The working modes and their specifications of the HEV model.

Number	HEV Working Mode	Specifications
1	veh_stop	Vehicle stops with engine and motor turned off
2	idle_nocharging	Idle condition for engine, no charging to battery
3	idle_charging	Idle condition for engine, charging to battery
4	brk_disablebrking	Mechanical brake
5	brk_enablebrking	Wheels drive motor to regenerate power, with mechanical brake being the assistance
6	cruise	Neither engine nor motor provides torque, the vehicle decelerates due to resistance
7	eDrive	The required torque was provided by motor only
8	LPM charging	The required torque was provided by engine, the engine works in optimized conditions, while the motor is charging the battery
9	eBoost	The required torque was provided by both engine and motor, the engine is working in optimized conditions, while the motor is charging the battery
10	ice_alone	The required torque was provided by engine only

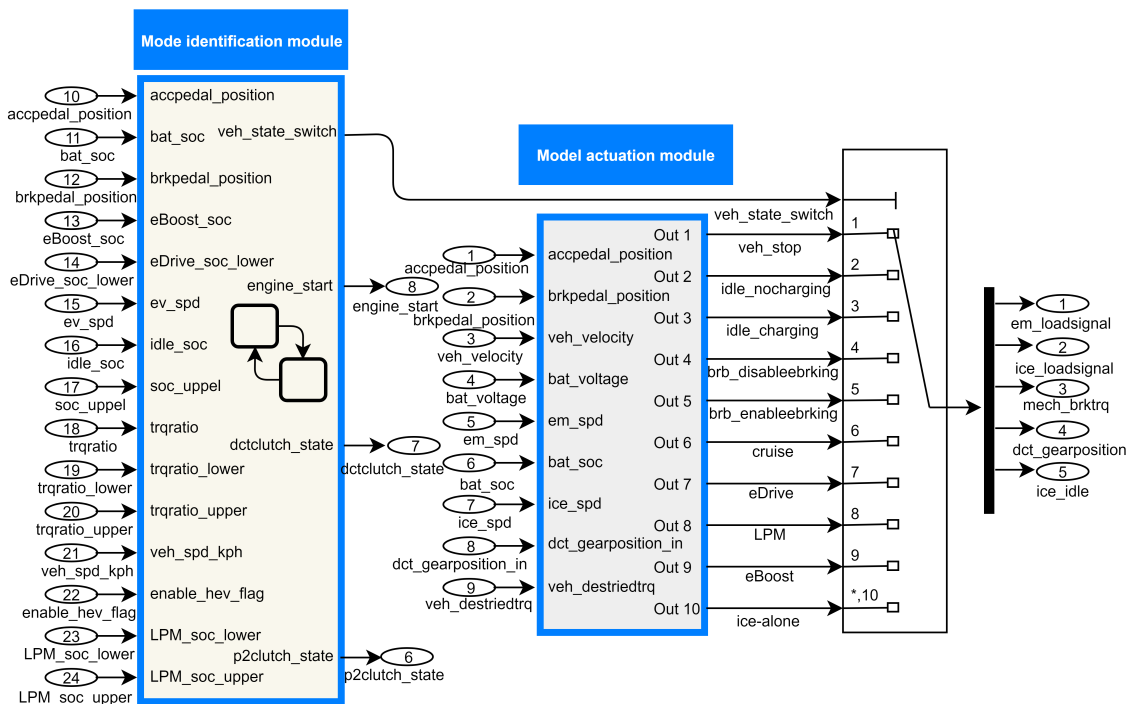


Figure 5. MATLAB/Simulink control strategy of the vehicle dynamic model presented in Figure 4.

2.3. Model Validation

The vehicle dynamic model was experimentally validated by the testing results of a PHEV SUV manufactured by the Shanghai Automotive Industry Cooperation (SAIC). The curb weight (dry weight) of vehicle is 2021 kg and the driving resistance coefficient A, B and C are 185.87 N, 1.0793 N/kph and 0.04899 N/kph², respectively. The vehicle also equipped with a lithium-ion battery with a maximum battery capacity of 8.8 kWh. The engine and motor characteristics are presented in Figure 6.

In this study, we calculated the fuel (gasoline) consumption of CVs under eight different driving cycles from year 2018 to 2040. Due to the development of advanced engine technology, the improvement of engine efficiency over the years needs to be considered. The current research follows the prediction from the Energy-saving and New Energy Vehicle Technology Roadmap released by China [32], and assumes a maximum engine efficiency of 38% for 2018, 40% for 2020, 50% for

2030 and 55% for 2040. Linear interpolation was employed to determine the engine efficiency for the years in between. In addition, the efficiency from the whole engine characteristic map (Figure 6a) was assumed to proportionally increase with the maximum efficiency. It should be noted that the engine characteristic map shown in Figure 6a has a maximum engine efficiency of 33% because it is not the most up-to-date engine model. In contrast, the efficiency of the motor is assumed to be constant over the years because the current motor efficiency is considered to be high enough with limited space for improvement. Therefore, the decrease of CO₂ emission for EV over the years is purely due to the reduced CO₂ emission from the power grid.

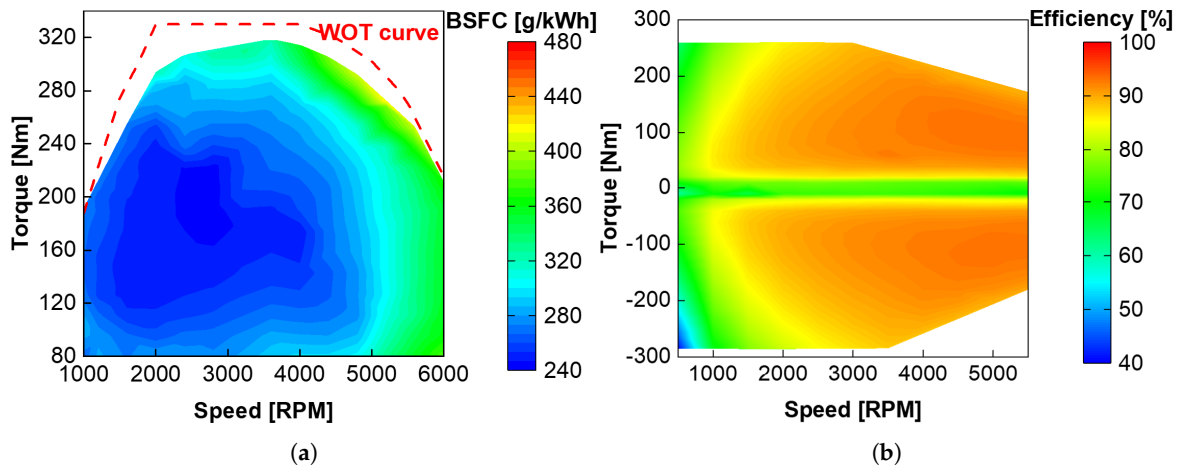


Figure 6. (a) engine and (b) motor characteristics of the hybrid electric vehicle employed in the current study.

The experiments follow the NEDC, with details shown in the following section. For the model validation, two conditions were studied—CV and P2 HEV. Under CV condition, both start and end SOC is 70, and the working modes experienced are 1, 2, 4 and 10 from Table 1. The battery did not discharge when the vehicle was driven by engine. The SOC of the vehicle therefore remained unchanged when operated in CV mode. However, for the P2 HEV condition, the start and end SOC are 63.0 and 64.5, respectively, and the working modes experienced include 1, 2, 5, 7, 8, 10. The results show that the deviation between the simulated and tested gasoline consumption (L/100 km) is within 3% under both CV and P2 HEV conditions. Considering that the HEV used in this study can be operated as pure EV or CV, in two extreme cases, this implies that our model is capable of capturing characteristics of the engine and motor modes of the vehicle. Therefore, the current vehicle dynamic model is considered to be accurate and valid to carry on the following analysis on CO₂ emission of CV and EV under various driving cycles for different countries. The starting SOC for the EV mode used in the model is 100% and a single cycle was run. The experimental conditions and specifications are summarized in Table 2.

Table 2. Conditions and specifications for model validation.

	CV	P2 HEV
Start SOC	70.0	63.0
End SOC	70.0	64.5
Working modes experienced	1, 2, 4, 10	1, 2, 5, 7, 8, 10
Gasoline consumption (L/100km)	9.733	6.975
Deviation between the simulation and experiments	< 3%	< 3%

2.4. Description of Driving Cycles

Figure 7 presents the dynamic characteristics of eight most commonly used driving cycles, including US06, HWFET, NEDC, UDSS, JC08, NYCC, CCUR and CCEW. Among them, US06 and HWFET are both used to indicate high-speed driving conditions. It can be seen from Figure 7a,b that US06 has greater vehicle acceleration/deceleration and peak vehicle speed. However, HWFET can be considered as a relatively stable highway operating condition with a maximum speed of no more than 96 km/h [33].

NEDC is a synthetic driving cycle that includes four repeating urban driving cycles and an extra-urban driving cycle. It is considered as the most robust driving cycle [33], i.e., vehicles based under the NEDC have the least degradation in performance than other driving cycles. However, the NEDC has relatively less dynamic changes compared with the other cycles described. In addition, in China’s national standards GB/T 18386-2005 and GB/T 19233-2008, the NEDC is used to measure the mileage, emission level and fuel consumption of vehicles (including CV and EV).

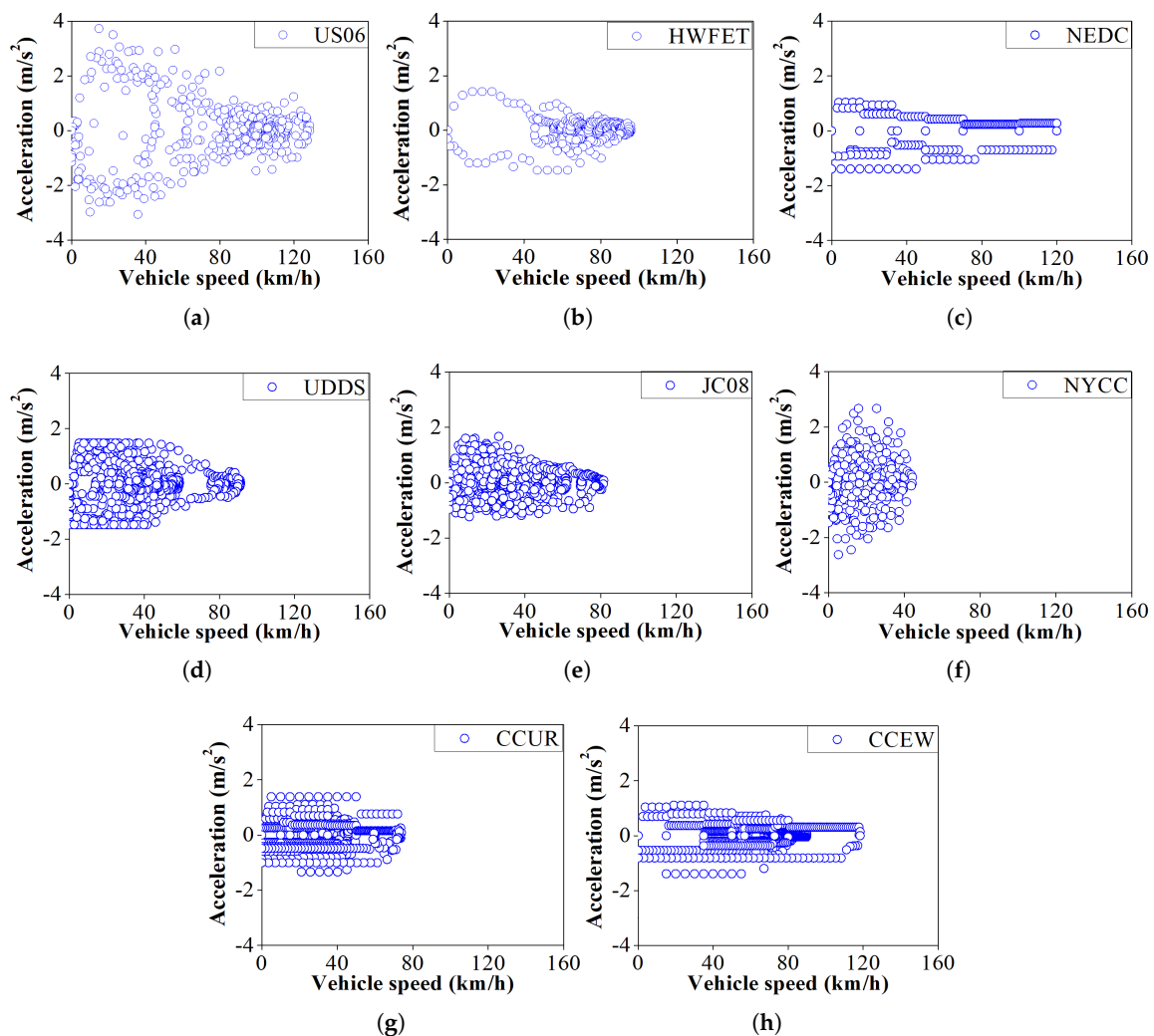


Figure 7. The dynamic characteristics of driving cycles based on acceleration and speed for: (a) US06; (b) HWFET; (c) NEDC; (d) UDSS; (e) JC08; (f) NYCC; (g) CCUR; and (h) CCEW.

In the US, the UDSS standard cycle is commonly used to evaluate the performance of light vehicles in urban conditions [24]. The widely-known FTP-75 driving cycle comes from UDSS, by adding the first 505 s of UDSS to its end. The JC08 driving cycle is a new fuel consumption and emissions test evaluation standard cycle implemented in Japan in 2015. It mainly reflects the characteristics of

crowded urban driving conditions. Compared with the previously used Japan 10–15 mode driving cycle, JC08 has longer mileage and more stringent acceleration/deceleration.

NYCC represents the driving conditions in urban centers with frequent starts and stops. It can be found from Figure 7f that the peak speed is the lowest among all driving cycles, but the maximum acceleration/deceleration is large, only slightly smaller than that of US06. In contrast with HWFET, NYCC represents the low speed/high acceleration driving conditions, while HWFET cycle stands for the high speed/low acceleration driving conditions.

Finally, this study also selected two urban circulation conditions with Chinese traffic characteristics, i.e., CCUR and CCEW. Expressway is defined as conditions with a vehicle speed of more than 60 km/h and no traffic lights, for instance the city ring of Beijing and Shanghai, etc. [25], while the speed on urban roads is significantly lower than that of expressways.

3. Results and Discussion

In this study, the CO₂ emissions (kg/100 km) of CV (fueled by gasoline) and EV of different countries/regions from year 2018 to 2040 were predicted. Figure 8 presents the CO₂ emission from CV and EV of different countries under NEDC. It was chosen for comparing different countries' CO₂ emission because it is considered to have the least degradation in performance. It should be noted that the emission of CV is universal across the globe in this study, as it was calculated based vehicle fuel consumption. It can be seen in Figure 8 that, from year 2018 to 2040, CV has higher CO₂ emission than EV. For all the countries studied, China has the highest CO₂ emission for EV, around 50% of that from CV in Year 2018 and 66% of that from CV in Year 2040. However, carbon emission of EV from the EU remains at the lowest level (around 7 kg/100 km) in this time frame. Meanwhile, CO₂ emission of EV from Japan and the world average is in between that from China and the EU, and their differences are completely determined by the CO₂ emission of electricity (shown in Figure 2).

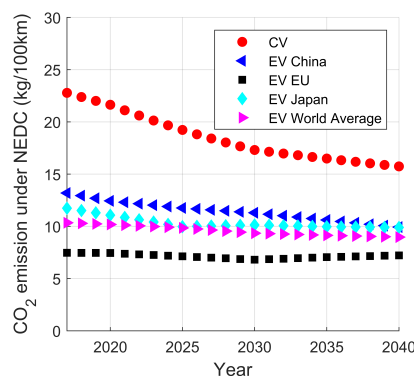


Figure 8. CO₂ emission of CV and EV under New European Driving Cycle for different countries from year 2018 to 2040. The EV model has electricity regeneration during braking.

Figure 9 presents the simulated results under eight different driving cycles. Since EV emission of different countries follow the exact same trend with their electricity emissions (shown in Figure 2), the following figures only show the trend for China and the EU as the two extreme representatives. Although the results are dependent on driving cycles (road conditions), there are some common trends for all types of driving cycles studied—(1) The CO₂ emission decreases over the years for both CVs and EVs, due to the increased engine efficiency and increased fraction of renewable energy in the power grid, respectively; (2) For all countries/regions, CV has higher CO₂ emission than EV from year 2018 to 2040; (3) China has the highest CO₂ emission for EVs, attributed to its higher CO₂ emission of electricity, followed by Japan, the world average and the EU.

Comparing Figure 9a,b with the other subfigures, it can be observed that the CO₂ emissions of CV (red curve) under China-fast and HWFET cycle are significantly lower, and closer to the emission of EV than other driving cycles. Specifically, under China Fast condition, the CO₂ emission of CV

is about 23% and 17% higher than that of China EV with no electricity regeneration during braking (ebraking) in year 2018 and 2040, respectively. For HWFET, the CO₂ emission of CV is 16% higher than that of China EV with no ebraking in 2018, and this figure decreases to 9% by 2040. As described in the previous section, HWFET represents relatively stable highway operating conditions in the US, while China-fast represents the driving conditions in expressways with no traffic lights in China. Under these conditions, the engine operates at high speed, medium load (torque), where the brake specific fuel consumption is the lowest (engine efficiency highest), as shown in Figure 6a. This explains the lower CO₂ emission of CV under highway than other conditions.

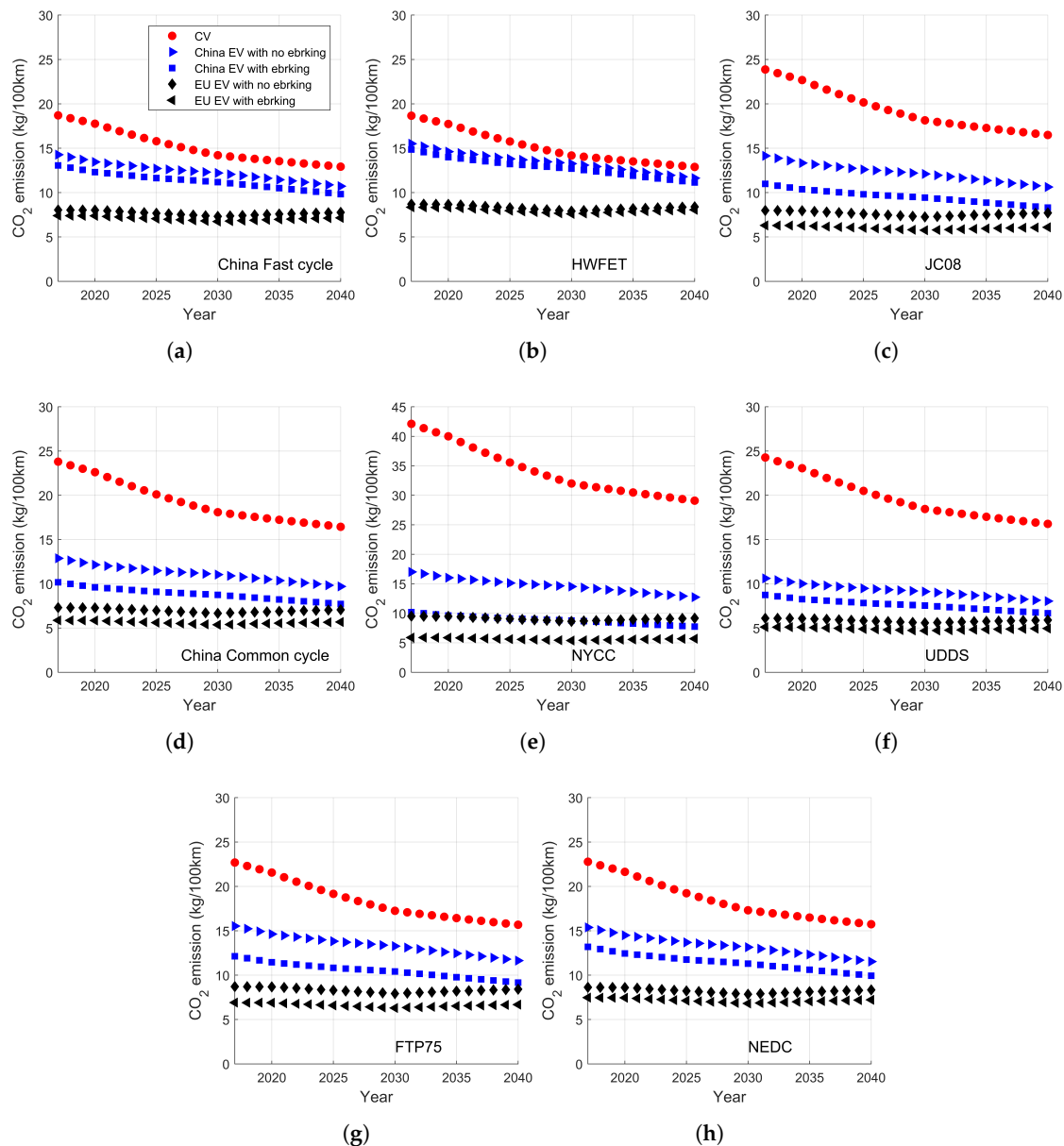


Figure 9. CO₂ emission from conventional vehicles fueled by gasoline and electric vehicles from China and the EU, predicted through 2040 under different driving conditions, including (a) China Fast cycle; (b) HWFET; (c) JC08; (d) China Common cycle; (e) NYCC; (f) UDDS; (g) FTP75 and (h) NEDC. ebraking means electricity regeneration during braking.

In contrast, in Figure 9c–g, the CO₂ emission of CV is a lot higher than that of EV. Among them, the most significant difference was observed in NYCC and UDDS cycle. For NYCC, the emission of

CV is 59% higher than that of China EV with no ebraking in 2018, and this difference is only slightly reduced to 56% in 2040, while that, for the UDDS cycle is 56% and 52%, respectively. This is because NYCC represents the driving conditions in urban centers with frequent starts and stops. UDDS is also used to evaluate the performance of light vehicles in urban conditions. On the other hand, JC08, China Common and FTP-75 cycle are standards for crowded urban driving conditions in Japan, China and the US, respectively. It can be seen from Figure 7a that, under these driving conditions, the vehicles maintain a low speed most of the time with frequent and significant acceleration and deceleration, which prohibits the engine from operating at its high efficiency regime (Figure 6a). Therefore, the CO₂ emission of CV is a lot higher than that of EV under these crowded urban conditions. The carbon emission of NEDC (Figure 9h) is similar to that under FTP-75 (Figure 9g). Additionally, it is found that the difference between EV with and without ebraking is larger in these urban driving conditions. This is because the frequent and substantial deceleration in the urban area recovers more electricity than other driving conditions. Therefore, it is suggested to activate ebraking for urban driving conditions in order to reduce carbon emission. Although it was found that EVs generally have less well-to-wheel CO₂ emissions across different driving cycles as well as countries/regions than CVs, it should be noted that EV growth can lead to potential reshaping of the electricity load curve as well as increasing total electricity demand, which can place new strains on the grid in near to midterm, and in the long run, respectively [34]. While the impact of power-demand of the EVs on the grid as well as its corresponding emission characteristics is important and warrants additional research, the topic itself is complex and is beyond the scope of this study.

4. Conclusions

This work predicted the well-to-wheel CO₂ emission of gasoline vehicle and electric vehicles for China, Europe, Japan and World Average through year 2040 under eight different driving conditions. An experimentally validated vehicle dynamic model was employed to calculate the gasoline and electricity consumption of CV and EV. The key conclusions are as follows:

1. The CO₂ emission decreases over the years for both CVs and EVs, due to the increased engine efficiency and increased fraction of renewable energy in the power grid, respectively.
2. For all the countries/regions studied, CVs have higher CO₂ emission than EVs from year 2018 to 2040.
3. For all the countries/regions studied, China has the highest CO₂ emission for EVs, followed by Japan, the world average, and the EU. Their differences are determined by CO₂ emission of electricity supply chain.
4. The difference of CO₂ emission from CVs and EVs is smaller under highway conditions, compared with those under urban driving conditions. For instance, the CO₂ emission from CVs is 23% higher than that of EVs in China in year 2018, and decreases to 17% in year 2040 for China-fast driving conditions.
5. For urban driving conditions, e.g., New York City Cycle, the carbon emission gap between CVs and EVs in China is 59% and 56% in year 2018 and year 2040, respectively. However, electricity regeneration during braking is found to be effective in reducing carbon emission for EVs under urban driving conditions.

Author Contributions: Conceptualization, X.D. and B.W.; Formal analysis, B.W. and Q.N.C.; Methodology, X.D. and B.W.; Resources, H.L.Y. and Q.N.C.; Validation, X.D. and B.W.; Visualization, X.D. and H.L.Y.; Writing—original draft, X.D.; Writing—review and editing, H.L.Y. and Q.N.C. All authors have read and agreed with the final manuscript.

Funding: This research was funded by China Postdoctoral Science Foundation Grant No. 2016M600313, as well as Talent Plan Research Supporting Funds from Shanghai Jiao Tong University.

Conflicts of Interest: The authors declare no conflict of interest.

Abbreviations

The following abbreviations are used in this manuscript:

CVs	Conventional vehicles
EVs	Electric vehicles
HEV	Hybrid electric vehicle
PHEV	Plug-in hybrid electric vehicle
HWFET	High way fuel economy test
UDDS	Urban dynamometer driving schedule
NYCC	New York city cycle
NEDC	New European driving cycle
CCUR	Chinese city driving cycle for urban road
CCEW	Chinese city driving cycle for express way
DCT	Dual clutch transmission
SOC	State of charge
ebraking	Electricity regeneration during braking

References

- O'Neill, B.C.; Oppenheimer, M. Dangerous climate impacts and the kyoto protocol. *Science* **2008**, *296*, 1971–1972. [[CrossRef](#)]
- Klein, R.J. Identifying countries that are particularly vulnerable to the adverse effects of climate change: An academic or a political challenge? *CCRC* **2009**, *3*, 284–291. [[CrossRef](#)]
- Takeshita, T. Assessing the co-benefits of CO₂ mitigation on air pollutants emissions from road vehicles. *Appl. Energy* **2012**, *97*, 225–237. [[CrossRef](#)]
- Rogelj, J.; Elzen, M.D.; Höhne, N.; Fransen, T.; Fekete, H.; Winkler, H.; Schaeffer, R.; Sha, F.; Riahi, K.; Meinshausen, M. Paris Agreement climate proposals need a boost to keep warming well below 2 °C. *Nature* **2016**, *534*, 631–639. [[CrossRef](#)]
- United Nations. *Paris Agreement*; United Nations: New York, NY, USA, 2015.
- Hoffert, M.I.; Caldeira, K.; Benford, G.; Criswell, D.R.; Green, C.; Herzog, H.; Jain, A.K.; Kheshgi, H.S.; Lackner, K.S.; Lewis, J.S.; et al. Advanced technology paths to global climate stability: Energy for a greenhouse planet. *Science* **2002**, *398*, 981–987. [[CrossRef](#)]
- International Energy Outlook 2017*; U.S. Energy Information Administration: Washington, DC, USA, 2017.
- Wang, D.; Zamel, N.; Jiao, K.; Zhou, Y.; Yu, S.; Du, Q.; Yin, Y. Life cycle analysis of internal combustion engine, electric and fuel cell vehicles for China. *Energy* **2013**, *59*, 402–412. [[CrossRef](#)]
- Bitonto, S.; Rico, T. *Electromobility in Germany: Vision 2020 and Beyond*; Germany Trade & Invest: Berlin, Germany, 2015.
- Lin, B.; Ouyang, X. Energy demand in China: Comparison of characteristics between the US and China in rapid urbanization stage. *Energy Convers. Manag.* **2014**, *79*, 128–139. [[CrossRef](#)]
- Hu, X.; Chang, S.; Li, J.; Qin, Y. Energy for sustainable road transportation in China: Challenges, initiatives and policy implications. *Energy* **2010**, *35*, 4289–4301. [[CrossRef](#)]
- Wang, Z.; Jin, Y.; Wang, M.; Wu, W. New fuel consumption standards for Chinese passenger vehicles and their effects on reductions of oil use and CO₂ emissions of the Chinese passenger vehicle fleet. *Energy Policy* **2010**, *38*, 5242–5250. [[CrossRef](#)]
- Hao, H.; Ou, X.; Du, J.; Wang, H.; Ouyang, M. China's electric vehicle subsidy scheme: Rationale and impacts. *Energy Policy* **2014**, *73*, 722–732. [[CrossRef](#)]
- Hao, H.; Wang, H.; Ouyang, M. Comparison of policies on vehicle ownership and use between Beijing and Shanghai and their impacts on fuel consumption by passenger vehicles. *Energy Policy* **2011**, *39*, 1016–1021. [[CrossRef](#)]
- Howey, D.A.; Martinez-Botas, R.F.; Cussons, B.; Lytton, L. Comparative measurements of the energy consumption of 51 electric, hybrid and internal combustion engine vehicles. *Transp. Res. Part D* **2011**, *16*, 459–464. [[CrossRef](#)]

16. Chan, Q.N.; Fattah, I.M.R.; Zhai, G.; Yip, H.L.; Chen, T.B.Y.; Yuen, A.C.Y.; Yang, W.; Wehrfritz, A.; Dong, X.; Kook, S.; et al. Color-ratio pyrometry methods for flame–wall impingement study. *J. Energy Inst.* **2018**, in press. [[CrossRef](#)]
17. Ming, C.; Fattah, I.M.R.; Chan, Q.N.; Pham, P.X.; Medwell, P.R.; Kook, S.; Yeoh, G.H.; Hawkes, E.R.; Masri, A.R. Combustion characterization of waste cooking oil and canola oil based biodiesels under simulated engine conditions. *Fuel* **2018**, *224*, 167–177. [[CrossRef](#)]
18. Fattah, I.M.R.; Ming, C.; Chan, Q.N.; Wehrfritz, A.; Pham, P.X.; Yang, W.; Kook, S.; Medwell, P.R.; Yeoh, G.H.; Hawkes, E.R.; et al. Spray and combustion investigation of post injections under low-temperature combustion conditions with biodiesel. *Energy Fuels* **2018**, *32*, 8727–8742, 167–177. [[CrossRef](#)]
19. Sullivan, J.L.; Hu, J. *Life Cycle Energy Analysis for Automobiles*; SAE Technical Paper No. 951829; SAE International: Warrendale, PA, USA, 1995.
20. Samaras, C.; Meisterling, K. Life cycle assessment of greenhouse gas emissions from plug-in hybrid vehicles: Implications for policy. *Environ. Sci. Technol.* **2008**, *42*, 3170–3176. [[CrossRef](#)]
21. Hao, H.; Wang, H.; Ouyang, M. Fuel conservation and GHG (greenhouse gas) emissions mitigation scenarios for China’s passenger vehicle fleet. *Energy* **2011**, *36*, 6520–6528. [[CrossRef](#)]
22. Peng, B.; Fan, Y.; Xu, J. Integrated assessment of energy efficiency technologies and CO₂ abatement cost curves in China’s road passenger car sector. *Energy Convers. Manag.* **2016**, *109*, 195–212. [[CrossRef](#)]
23. Plotkin, S.; Singh, M.; Patterson, P.; Ward, J.; Wood, F.; Kydes, N.; Holte, J.; Moore, J.; Miller, G.; Das, S.; et al. *Multi-Path Transportation Futures Study: Vehicle Characterization and Scenario Analyses: Main Text and Appendices A, B, C, D, and F*; Argonne National Laboratory: Argonne, IL, USA, 2009.
24. Dynamometer Drive Schedules. Available online: <https://www.epa.gov/vehicle-and-fuel-emissions-testing/dynamometer-drive-schedules> (accessed on 15 February 2019).
25. *City Driving Cycle for Vehicle Testing*; National Development and Reform Commission of the People’s Republic of China: Beijing, China, 2006.
26. Bao, Y.; Chan, Q.N.; Kook, S.; Hawkes, E. Spray penetrations of ethanol, gasoline and iso-octane in an optically accessible spark-ignition direct-injection engine. *SAE Int. J. Fuels Lubr.* **2014**, *7*, 1010–1026. [[CrossRef](#)]
27. Zhao, F.; Lai, M.C.; Harrington, D.L. Automotive spark-ignited direct-injection gasoline engines. *Prog. Energy Combust. Sci.* **1999**, *25*, 437–562. [[CrossRef](#)]
28. Chan, Q.N.; Bao, Y.; Kook, S. Effects of injection pressure on the structural transformation of flash-boiling sprays of gasoline and ethanol in a spark-ignition direct-injection (SIDI) engine. *Fuel* **2014**, *130*, 228–240. [[CrossRef](#)]
29. Yang, J.; Xu, M.; Hung, D.L.S.; Wu, Q.; Dong, X. Influence of swirl ratio on fuel distribution and cyclic variation under flash boiling conditions in a spark ignition direct injection gasoline engine. *Energy Convers. Manag.* **2017**, *138*, 565–576. [[CrossRef](#)]
30. Yang, J.; Dong, X.; Wu, Q.; Xu, M. Influence of flash boiling spray on the combustion characteristics of a spark-ignition direct-injection optical engine under cold start. *Combust. Flame* **2018**, *188*, 66–76. [[CrossRef](#)]
31. Hitomi, M. *Our Direction for ICE*; The Japan Society of Mechanical Engineers: Tokyo, Japan, 2017.
32. Weng, S. “Jieneng Yu Xin Nengyuan Qiche Jishu Luxiantu” Zhengshi Fabu. *Qiche Yu Peijian* **2016**, *46*, 30–31.
33. Whitefoot, J.W.; Ahn, K.; Papalambros, P.Y. The case for urban vehicles: Powertrain optimization of a power-split hybrid for fuel economy on multiple drive cycles. In Proceedings of the ASME 2010 International Design Engineering Technical Conferences & Computers and Information in Engineering Conference, Montreal, QC, Canada, 15–18 August 2010.
34. *The Potential Impact of Electric Vehicles on Global Energy Systems*; McKinsey & Co.: New York, NY, USA, 2018.

